Two-loop radiative corrections in $b \to s\,(l^+ l^-)$ decays

Adrian Ghinculov U. of Rochester

Tobias Hurth CERN

Gino Isidori Frascati

York-Peng Yao U. of Michigan

LoopFest II
Brookhaven National Laboratory
May 14-16, 2003

Overview

- Physics goals of future colliders: NLC, LHC, $\mu\mu$ …
  - Spontaneous symmetry breaking
  - Search for new physics
  - More precise measurements of EW parameters
- Need for multi-leg, higher-loop radiative corrections which can be included in Monte Carlo simulations

$b \Rightarrow s\ (l^+ l^-)$

- Experimentally, B physics is in high gear:

  - Experimental situation in B physics:

Babar	1999	e^+e^-	Tevatron II	2001	$p\bar{p}$
Belle	1999	e^+e^-	LHC	2007	pp
CLEO III	2000	e^+e^-	BTeV	2007	$p\bar{p}$

- Leading order is 1-loop penguin diagrams:

  - Rare B decays like $B \to X_{s,d}\gamma$ or $B \to X_s \ell^+\ell^-$ directly probe the SM at the quantum level.

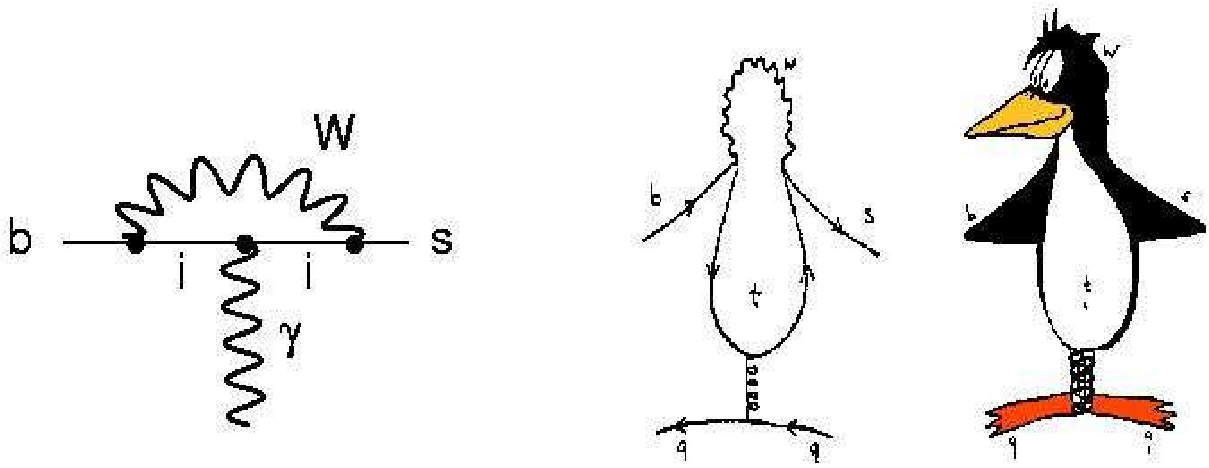

$\Rightarrow$ High sensitivity to nonstandard contributions
(2HDM : charged Higgs; MSSM : chargino, gluino....)
. Indirect search for new physics

- Existing experimental data:

Dimuon mass distribution of $B \to K\mu^+\mu^-$ candidates:

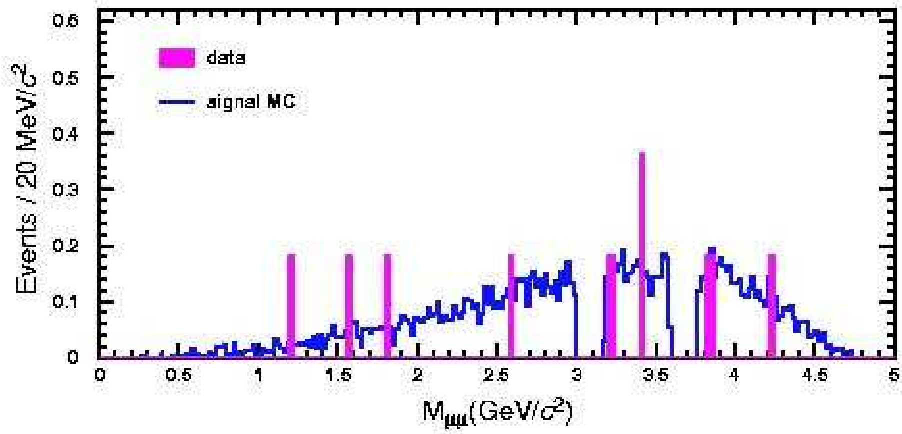

- Theoretically, there are two perturbative windows separated by the c cbar resonances:

- On-shell $c\bar{c}$ resonances:

  $\Rightarrow$ kinematical cuts in the dilepton mass spectrum necessary: two perturbative windows:

  $0.05 < (m_{l^+l^-}/m_b)^2 < 0.25$ and $0.65 < (m_{l^+l^-}/m_b)^2$

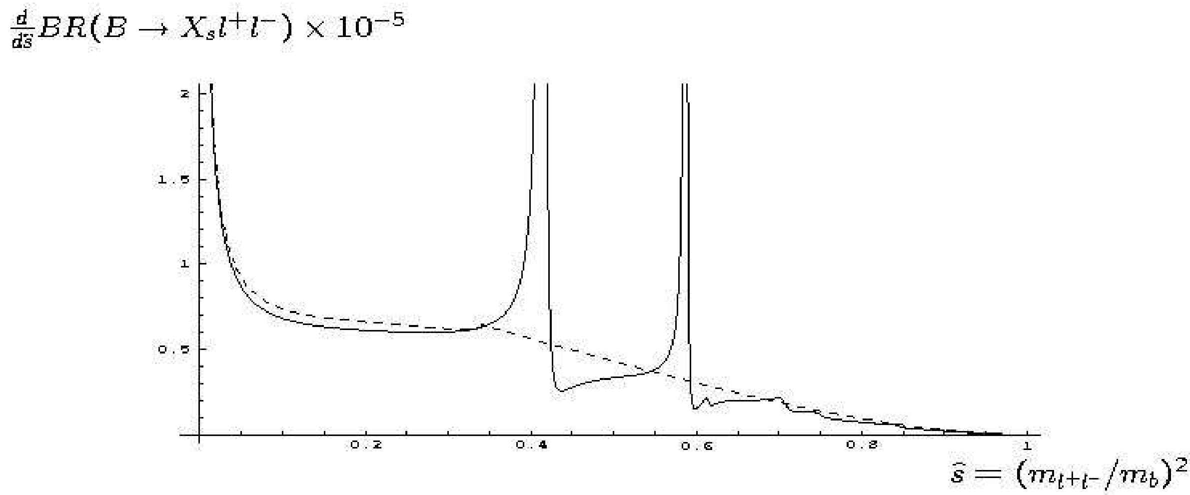

- It would be nice to have a program to calculate the 2-loop corrections for any combination of kinematic parameters with a mouse click:

$B \to s\,\gamma^*$

Penguin.V3.exe

- QCD radiative corrections are available in the low s region by expansion techniques

  H.H. Asatryan, H.M. Asatryan,
  C. Greub, and M. Walker

- Bremsstrahlung is available

  A.G., T. Hurth, G. Isidori, Y.-P. Yao
  Asatryan *et al*.

- The virtual correction diagrams can be organized in five gauge invariant subsets:

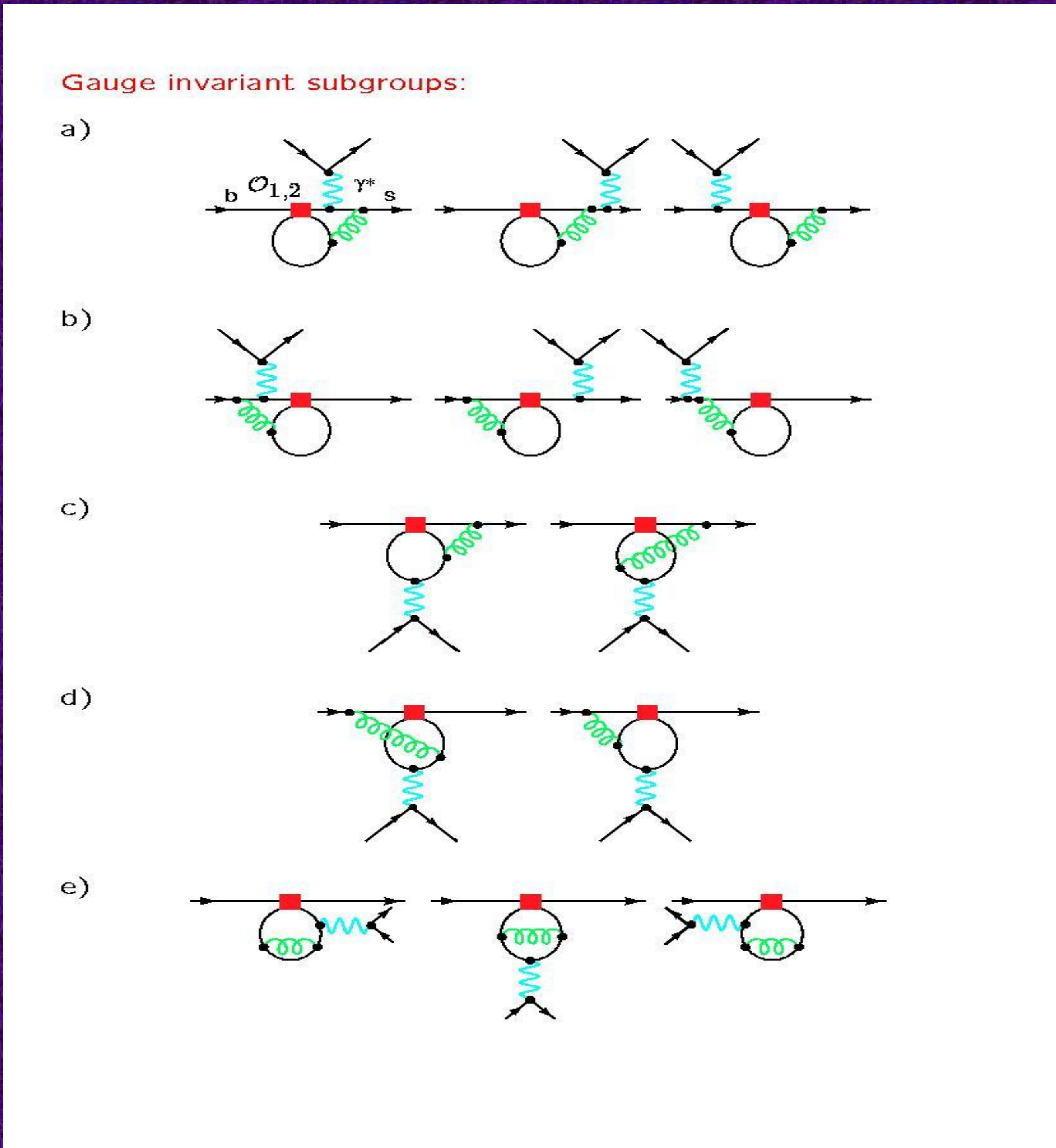

Two-loop radiative corrections

- Special cases of 2-loop diagrams
  - Zero mass diagrams: QCD, QED
    - 2-loop Bhabha scattering

      Z. Bern, L. Dixon, A. G.
    - Light-by-light scattering

      Z. Bern, A. De Freitas, L. Dixon, A. G., and H.C. Wong
    - All QCD $2 \to 2$ scattering processes

      Z. Bern, L. Dixon, D. A. Kosower

      C. Anastasiou, N. Glover, C. Oleari, and M.E. Tejeda-Yeomans
  - Vacuum diagrams are always expressible in terms of Spence functions. Complete solution due to J.J. van der Bij and M. Veltman (1984).

- In the general kinematic case lead to extremely complicated and often unknown functions

e.g. the 2-loop sunset diagram

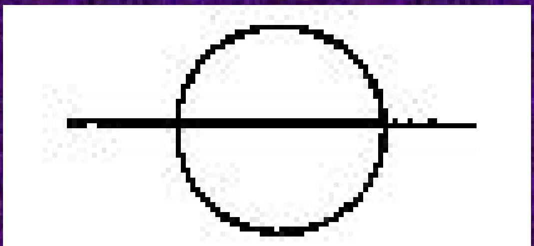

is expressed in terms of Lauricella (1888) functions (generalized hypergeometric functions) Berends *et al.* '92

- => Hybrid analytic-numerical approach

A. G., J.J. van der Bij, Y.-P. Yao

Caveat: I.R. singularities need to be extracted analytically before numerical integration

- Analytical tensor reduction
  - Feynman parameters
  - Dirac algebra
  - Tensor decomposition
  - Recursion relations
  - Set of 10 scalar functions h_i
  - *=> complicated formulae*
- Numerical integration
  - Automatic singularity finding
  - Automatic complex integration path
  - High precision numerical integration algorithm for h_i
  - Final multi-dimensional integration by using an adaptative deterministic integration algorithm
  - *=> grid of integration points covering the whole relevant kinematic range*
- Final product
  - Fast interpolation program that can be integrated into MC simulations
  - *=> fast 2-loop evaluation*

Tensor decomposition

- Any 2-loop diagram looks like this:

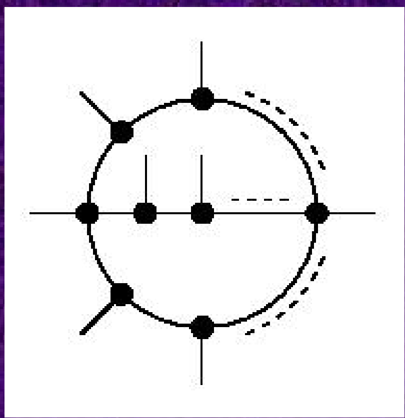

- This can always be expressed as an integral over sunset-type functions by introducing a number of Feynman parameters:

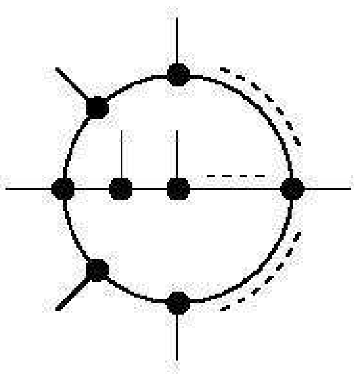

$$= \int_0^1 \int_0^1 \cdots \int_0^1 dX$$

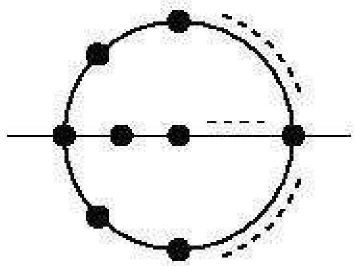

$$\int d^n p \, d^n q \, \frac{p^{\mu_1} \ldots p^{\mu_i} q^{\mu_{i+1}} \ldots q^{\mu_j}}{[(p+k)^2 + m_1^2]^{\alpha_1} \, (q^2 + m_2^2)^{\alpha_2} \, (r^2 + m_3^2)^{\alpha_3}} \quad .$$

- After tensor reduction this reduces to a set of 10 scalar integrals:

$$
\begin{aligned}
\mathcal{H}_1 &= \int d^n p\, d^n q\, \frac{1}{[(p+k)^2+m_1^2]^2\,(q^2+m_2^2)\,(r^2+m_3^2)} \\
\mathcal{H}_2 &= \int d^n p\, d^n q\, \frac{p\cdot k}{[(p+k)^2+m_1^2]^2\,(q^2+m_2^2)\,(r^2+m_3^2)} \\
\mathcal{H}_3 &= \int d^n p\, d^n q\, \frac{q\cdot k}{[(p+k)^2+m_1^2]^2\,(q^2+m_2^2)\,(r^2+m_3^2)} \\
\mathcal{H}_4 &= \int d^n p\, d^n q\, \frac{(p\cdot k)^2-\frac{1}{n}k^2p^2}{[(p+k)^2+m_1^2]^2\,(q^2+m_2^2)\,(r^2+m_3^2)} \\
\mathcal{H}_5 &= \int d^n p\, d^n q\, \frac{(p\cdot k)(q\cdot k)-\frac{1}{n}k^2(q\cdot p)}{[(p+k)^2+m_1^2]^2\,(q^2+m_2^2)\,(r^2+m_3^2)} \\
\mathcal{H}_6 &= \int d^n p\, d^n q\, \frac{(q\cdot k)^2-\frac{1}{n}k^2q^2}{[(p+k)^2+m_1^2]^2\,(q^2+m_2^2)\,(r^2+m_3^2)} \\
\mathcal{H}_7 &= \int d^n p\, d^n q\, \frac{(p\cdot k)^3-\frac{3}{n+2}k^2p^2(p\cdot k)}{[(p+k)^2+m_1^2]^2\,(q^2+m_2^2)\,(r^2+m_3^2)} \\
\mathcal{H}_8 &= \int d^n p\, d^n q\, \frac{(p\cdot k)^2(q\cdot k)-\frac{3}{n+2}k^2p^2(q\cdot k)}{[(p+k)^2+m_1^2]^2\,(q^2+m_2^2)\,(r^2+m_3^2)}
\end{aligned}
$$

$$
\begin{aligned}
\mathcal{H}_9 &= \int d^n p\, d^n q\, \frac{(p\cdot k)(q\cdot k)^2-\frac{1}{n+2}k^2[2(p\cdot q)(q\cdot k)+q^2(p\cdot k)]}{[(p+k)^2+m_1^2]^2\,(q^2+m_2^2)\,(r^2+m_3^2)} \\
\mathcal{H}_{10} &= \int d^n p\, d^n q\, \frac{(q\cdot k)^3-\frac{3}{n+2}k^2q^2(q\cdot k)}{[(p+k)^2+m_1^2]^2\,(q^2+m_2^2)\,(r^2+m_3^2)}
\end{aligned}
$$

- The UV divergences can be isolated as poles in $\varepsilon = n - 4$:

$$\mathcal{H}_1 = \pi^4 \left[\frac{2}{\epsilon^2} - \frac{1}{\epsilon}(1 - 2\gamma_{m_1}) - \frac{1}{2} + \frac{\pi^2}{12} - \gamma_{m_1} + \gamma_{m_1}^2 + h_1 \right]$$

$$\mathcal{H}_2 = \pi^4 k^2 \left[-\frac{2}{\epsilon^2} + \frac{1}{\epsilon}(\frac{1}{2} - 2\gamma_{m_1}) + \frac{13}{8} - \frac{\pi^2}{12} + \frac{\gamma_{m_1}}{2} - \gamma_{m_1}^2 - h_2 \right]$$

$$\mathcal{H}_3 = \pi^4 k^2 \left[\frac{1}{\epsilon^2} - \frac{1}{\epsilon}(\frac{1}{4} - \gamma_{m_1}) - \frac{13}{16} + \frac{\pi^2}{24} - \frac{\gamma_{m_1}}{4} + \frac{\gamma_{m_1}^2}{2} + h_3 \right]$$

$$\mathcal{H}_4 = \pi^4 (k^2)^2 \left[\frac{3}{2\epsilon^2} + \frac{1}{\epsilon}\frac{3\gamma_{m_1}}{2} - \frac{175}{96} + \frac{\pi^2}{16} + \frac{3\gamma_{m_1}^2}{4} + \frac{3}{4} h_4 \right]$$

$$\mathcal{H}_5 = \pi^4 (k^2)^2 \left[-\frac{3}{4\epsilon^2} - \frac{1}{\epsilon}\frac{3\gamma_{m_1}}{4} + \frac{175}{192} - \frac{\pi^2}{32} - \frac{3\gamma_{m_1}^2}{8} - \frac{3}{4} h_5 \right]$$

$$\mathcal{H}_6 = \pi^4 (k^2)^2 \left[\frac{1}{2\epsilon^2} - \frac{1}{\epsilon}(\frac{1}{24} - \frac{\gamma_{m_1}}{2}) - \frac{19}{32} + \frac{\pi^2}{48} - \frac{\gamma_{m_1}}{24} + \frac{\gamma_{m_1}^2}{4} + \frac{3}{4} h_6 \right]$$

$$\mathcal{H}_7 = \pi^4 (k^2)^3 \left[-\frac{1}{\epsilon^2} - \frac{1}{\epsilon}(\frac{5}{24} + \gamma_{m_1}) + \frac{287}{192} - \frac{\pi^2}{24} - \frac{5\gamma_{m_1}}{24} - \frac{\gamma_{m_1}^2}{2} - \frac{1}{2} h_7 \right]$$

$$\mathcal{H}_8 = \pi^4 (k^2)^3 \left[\frac{1}{2\epsilon^2} + \frac{1}{\epsilon}(\frac{5}{48} + \frac{\gamma_{m_1}}{2}) - \frac{287}{384} + \frac{\pi^2}{48} + \frac{5\gamma_{m_1}}{48} + \frac{\gamma_{m_1}^2}{4} + \frac{1}{2} h_8 \right]$$

$$\mathcal{H}_9 = \pi^4 (k^2)^3 \left[-\frac{1}{3\epsilon^2} - \frac{1}{\epsilon}(\frac{1}{24} + \frac{\gamma_{m_1}}{3}) + \frac{95}{192} - \frac{\pi^2}{72} - \frac{\gamma_{m_1}}{24} - \frac{\gamma_{m_1}^2}{6} - \frac{1}{2} h_9 \right]$$

$$\mathcal{H}_{10} = \pi^4 (k^2)^3 \left[\frac{1}{4\epsilon^2} + \frac{1}{\epsilon}(\frac{1}{96} + \frac{\gamma_{m_1}}{4}) - \frac{283}{768} + \frac{\pi^2}{96} + \frac{\gamma_{m_1}}{96} + \frac{\gamma_{m_1}^2}{8} + \frac{1}{2} h_{10} \right]$$

- The UV finite parts can be reduced to four building blocks and further integrated numerically:

$$
\begin{aligned}
h_1(m_1,m_2,m_3;k^2) &= \int_0^1 dx\, \bar{g}(x) \\
h_2(m_1,m_2,m_3;k^2) &= \int_0^1 dx\, [\bar{g}(x) + \bar{f}_1(x)] \\
h_3(m_1,m_2,m_3;k^2) &= \int_0^1 dx\, [\bar{g}(x) + \bar{f}_1(x)]\,(1-x) \\
h_4(m_1,m_2,m_3;k^2) &= \int_0^1 dx\, [\bar{g}(x) + \bar{f}_1(x) + \bar{f}_2(x)] \\
h_5(m_1,m_2,m_3;k^2) &= \int_0^1 dx\, [\bar{g}(x) + \bar{f}_1(x) + \bar{f}_2(x)]\,(1-x) \\
h_6(m_1,m_2,m_3;k^2) &= \int_0^1 dx\, [\bar{g}(x) + \bar{f}_1(x) + \bar{f}_2(x)]\,(1-x)^2 \\
h_7(m_1,m_2,m_3;k^2) &= \int_0^1 dx\, [\bar{g}(x) + \bar{f}_1(x) + \bar{f}_2(x) + \bar{f}_3(x)] \\
h_8(m_1,m_2,m_3;k^2) &= \int_0^1 dx\, [\bar{g}(x) + \bar{f}_1(x) + \bar{f}_2(x) + \bar{f}_3(x)]\,(1-x) \\
h_9(m_1,m_2,m_3;k^2) &= \int_0^1 dx\, [\bar{g}(x) + \bar{f}_1(x) + \bar{f}_2(x) + \bar{f}_3(x)]\,(1-x)^2 \\
h_{10}(m_1,m_2,m_3;k^2) &= \int_0^1 dx\, [\bar{g}(x) + \bar{f}_1(x) + \bar{f}_2(x) + \bar{f}_3(x)]\,(1-x)^3
\end{aligned}
$$

$$
\begin{aligned}
\bar{g}(m_1,m_2,m_3;k^2;x) &= Sp(\frac{1}{1-y_1}) + Sp(\frac{1}{1-y_2}) + y_1 \log\frac{y_1}{y_1-1} + y_2 \log\frac{y_2}{y_2-1} \\
\bar{f}_1(m_1,m_2,m_3;k^2;x) &= \frac{1}{2}\left[-\frac{1-\mu^2}{\kappa^2} + y_1^2 \log\frac{y_1}{y_1-1} + y_2^2 \log\frac{y_2}{y_2-1}\right] \\
\bar{f}_2(m_1,m_2,m_3;k^2;x) &= \frac{1}{3}\left[-\frac{2}{\kappa^2} - \frac{1-\mu^2}{2\kappa^2} - \left(\frac{1-\mu^2}{\kappa^2}\right)^2\right. \\
&\qquad \left. + y_1^3 \log\frac{y_1}{y_1-1} + y_2^3 \log\frac{y_2}{y_2-1}\right] \\
\bar{f}_3(m_1,m_2,m_3;k^2;x) &= \frac{1}{4}\left[-\frac{4}{\kappa^2} - \left(\frac{1}{3}+\frac{3}{\kappa^2}\right)\left(\frac{1-\mu^2}{\kappa^2}\right) - \frac{1}{2}\left(\frac{1-\mu^2}{\kappa^2}\right)^2 - \left(\frac{1-\mu^2}{\kappa^2}\right)^3\right. \\
&\qquad \left. + y_1^4 \log\frac{y_1}{y_1-1} + y_2^4 \log\frac{y_2}{y_2-1}\right]
\end{aligned}
$$

where we use the following notations:

$$
\begin{aligned}
y_{1,2} &= \frac{1+\kappa^2-\mu^2 \pm \sqrt{\Delta}}{2\kappa^2} \\
\Delta &= (1+\kappa^2-\mu^2)^2 + 4\kappa^2\mu^2 - 4i\kappa^2\eta
\end{aligned}
$$

and

$$
\begin{aligned}
\mu^2 &= \frac{ax + b(1-x)}{x(1-x)} \\
a &= \frac{m_2^2}{m_1^2}, \quad b = \frac{m_3^2}{m_1^2}, \quad \kappa^2 = \frac{k^2}{m_1^2}
\end{aligned}
$$

Efficient numerical integration

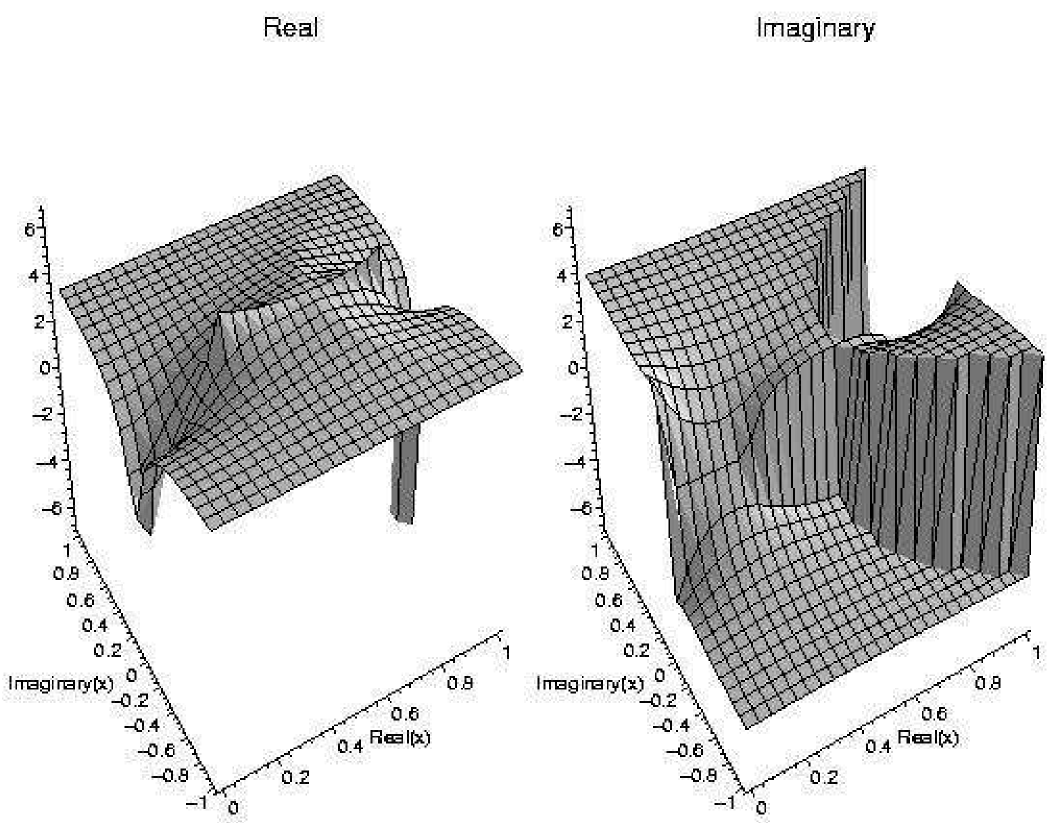

Typical behaviour of the functions $\tilde{g}(x)$, $\tilde{f}_1(x)$, $\tilde{f}_2(x)$, $\tilde{f}_3(x)$ and of their derivatives in the complex integration parameter x. The integration proceeds from $x = 0$ to $x = 1$.

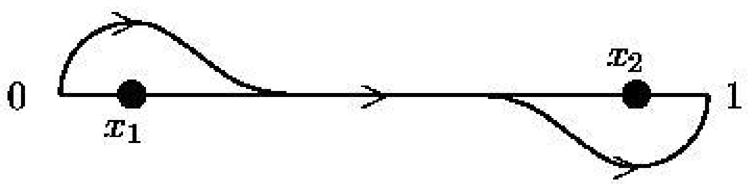

A typical shape for the complex integration path, defined in terms of higher order spline functions. Both the path and the Jacobian are smooth functions.

- After a 1-dimensional numerical integration, the h_i functions look like this:

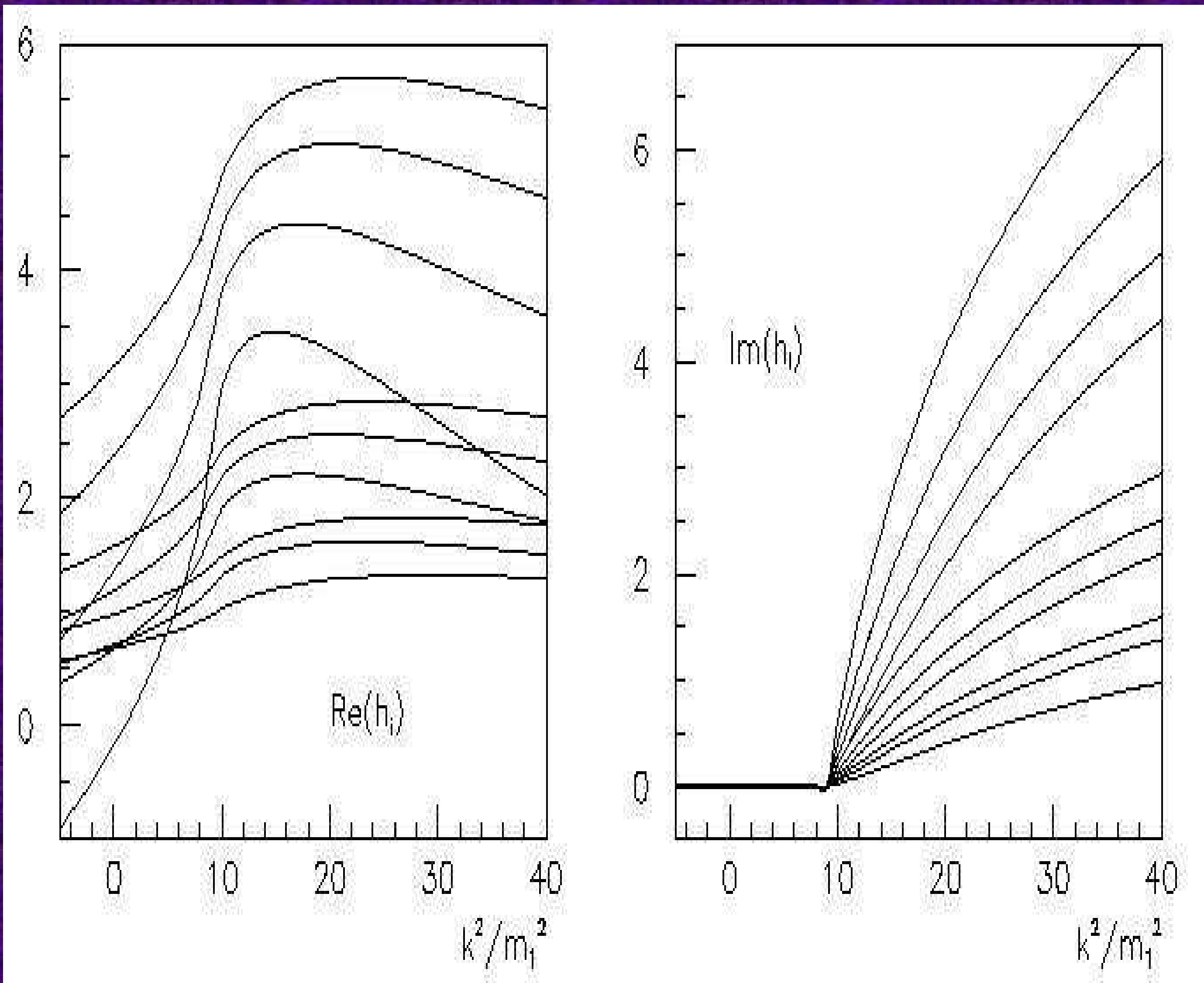

- The remaining Feynman parameter integrations are performed numerically by using the same techniques.

- Caveat: IR singularities need to be separated before numerical integration!

E.g. IR separation in Z ⇨ bbar

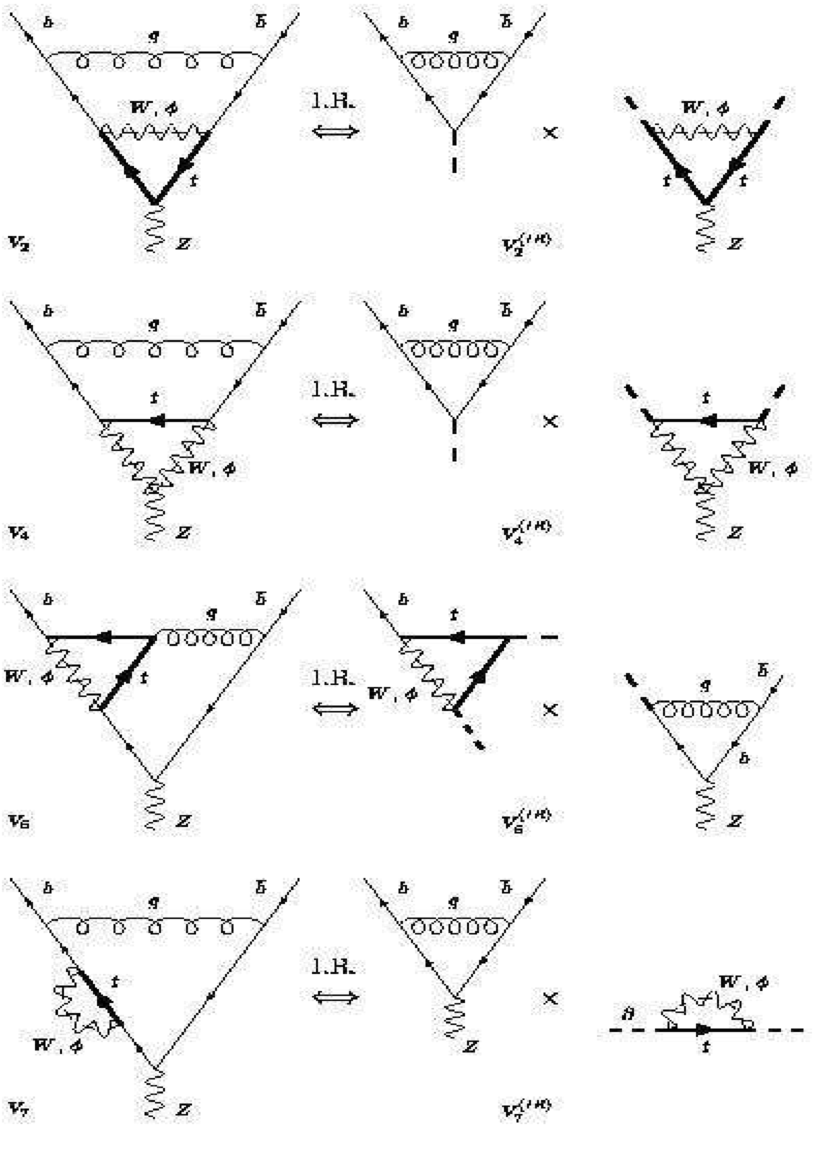

Figure 8: *Extracting the infrared divergent pieces of the two-loop diagrams analytically. The infrared divergency of the two-loop diagram is the same as the infrared divergency of the product of the two one-loop diagrams obtained by "freezing" the common line in the loop momenta integration.*

Tested on many other physical processes

- B physics — A.G., T. Hurth, G. Isidori, Y.-P. Yao
  - Full next-to-leading order QCD corrections to
    - b ⇨ s γ
    - b ⇨ s (l+l-)
- Top decay — A.G. and Y.-P. Yao
  - QCD corrections to the top quark width
- Z ->b bar — A.G. and Y.-P. Yao
  indirect top mass measurement at LEP and SLC
- Higgs physics — A.G. and J.J. van der Bij
  - Higgs decay into fermions: H ⇨ t tbar
  - main heavy Higgs decay mode: H ⇨ WW, ZZ
  - muon collider Higgs resonance shape:
    $\mu\mu$ ⇨ H ⇨ WW, ZZ
  - LHC gluon fusion resonance shape:
    gg ⇨ H ⇨ WW, ZZ

Computational challenges

- To be useful for comparing with the experiments, our results must cover three variables:
  - Charm mass
  - Dilepton invariant mass
  - Subtraction scale

- Grid containing 3 X 3 X 38 X 2 independent points calculated at 0.1% accuracy
  Intermediary points obtained by interpolation

- Huge computational problem

- Used the CERN Linux cluster:
  approx. 3 days running on 33 processors

- In the <u>low</u> dilepton invariant mass limit, we have a strong test of our results based on Asatryan et al. mass and momentum expansion results

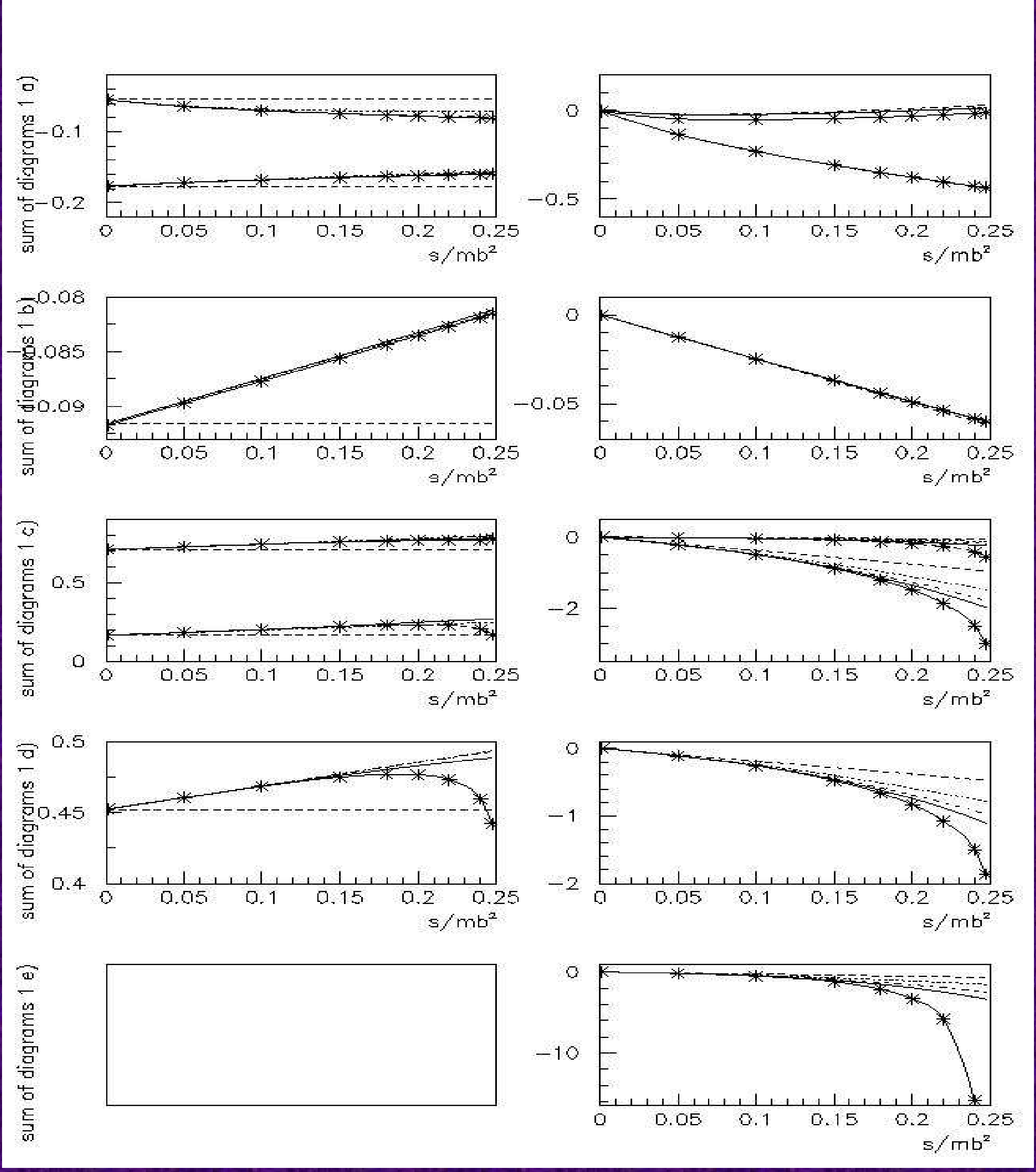

- For some graphs, the mass/momentum expansion works better…

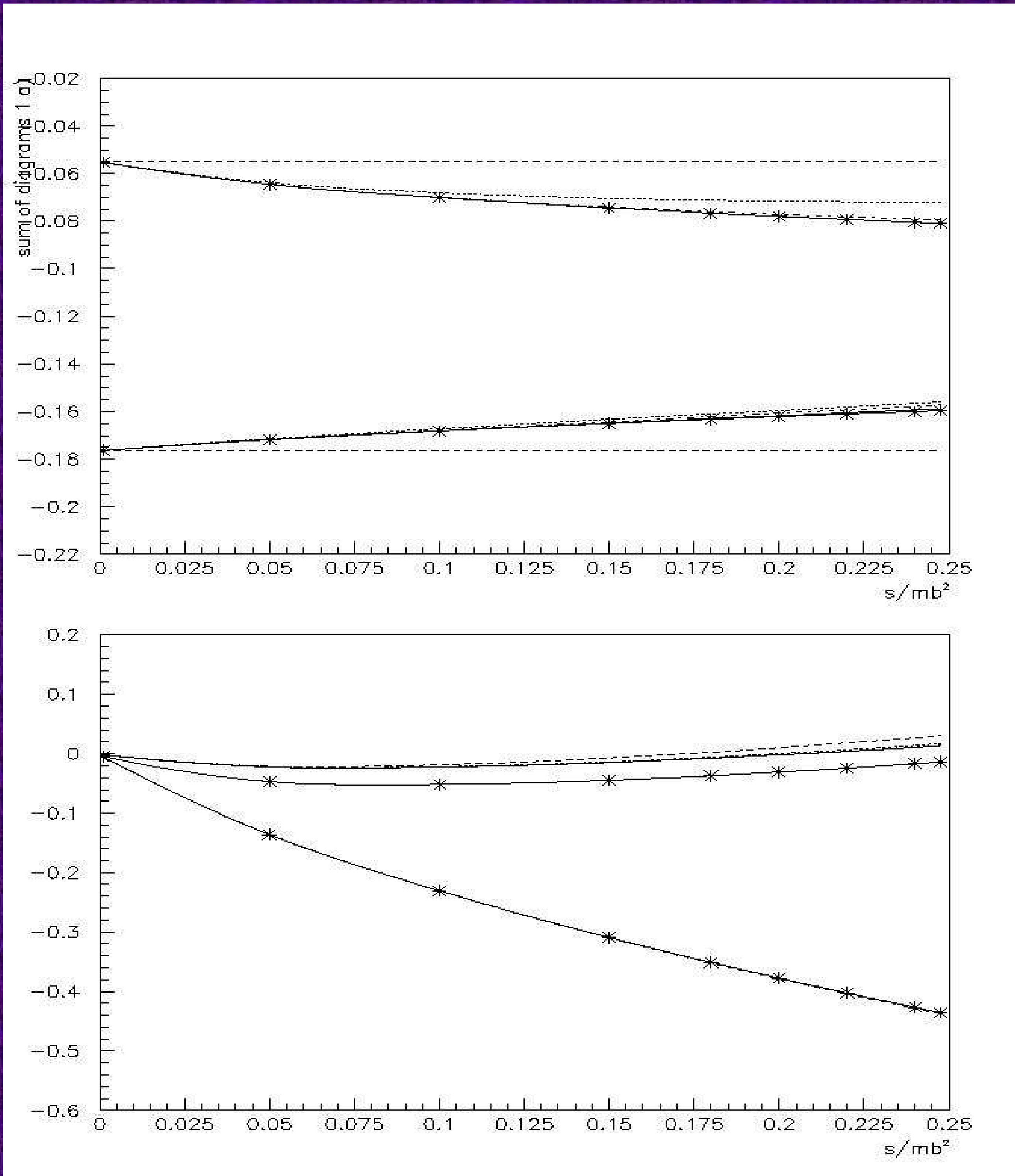

- … for other diagrams it works worse .

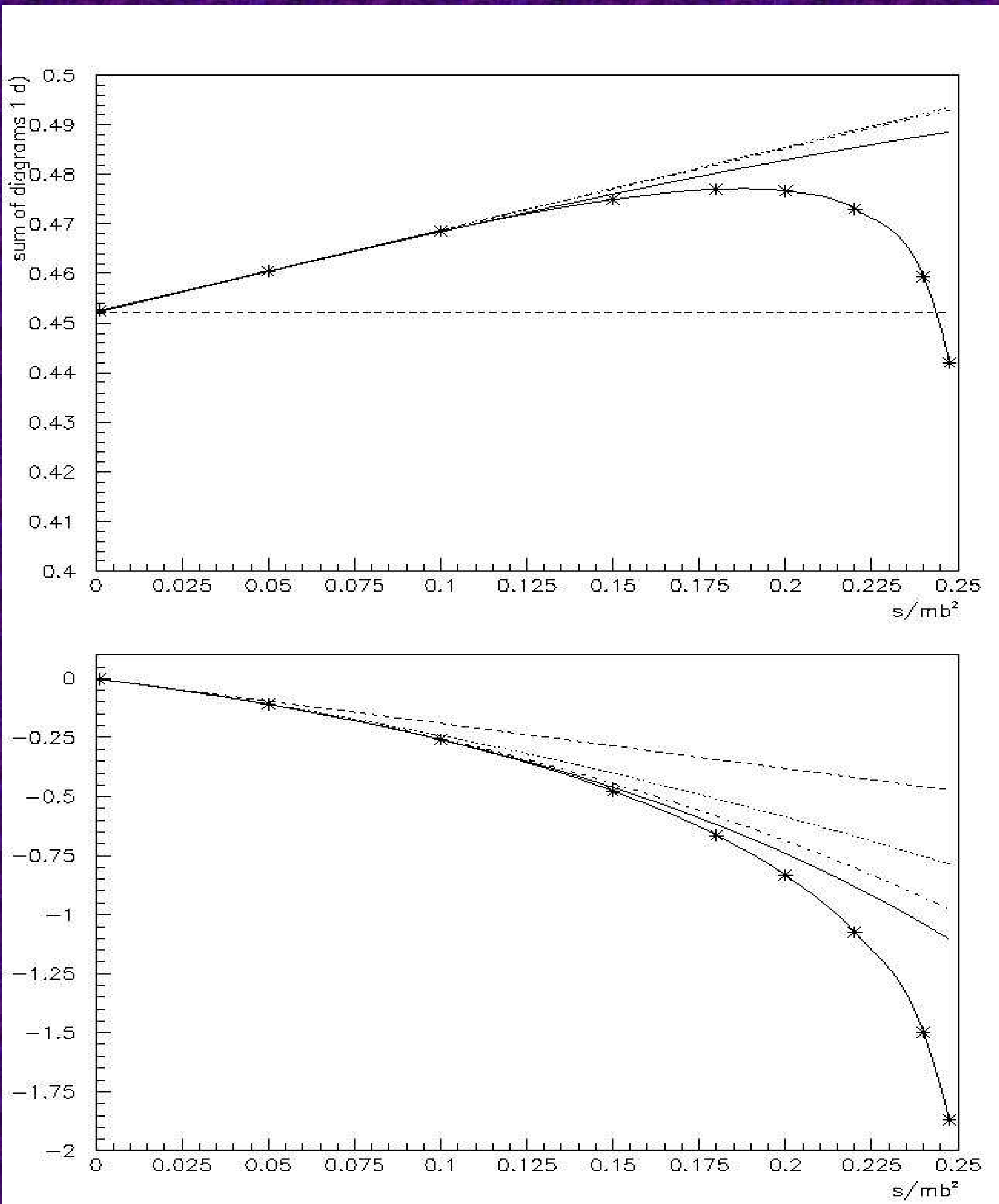

Numerical results valid over the whole kinematic range of the dilepton spectrum:

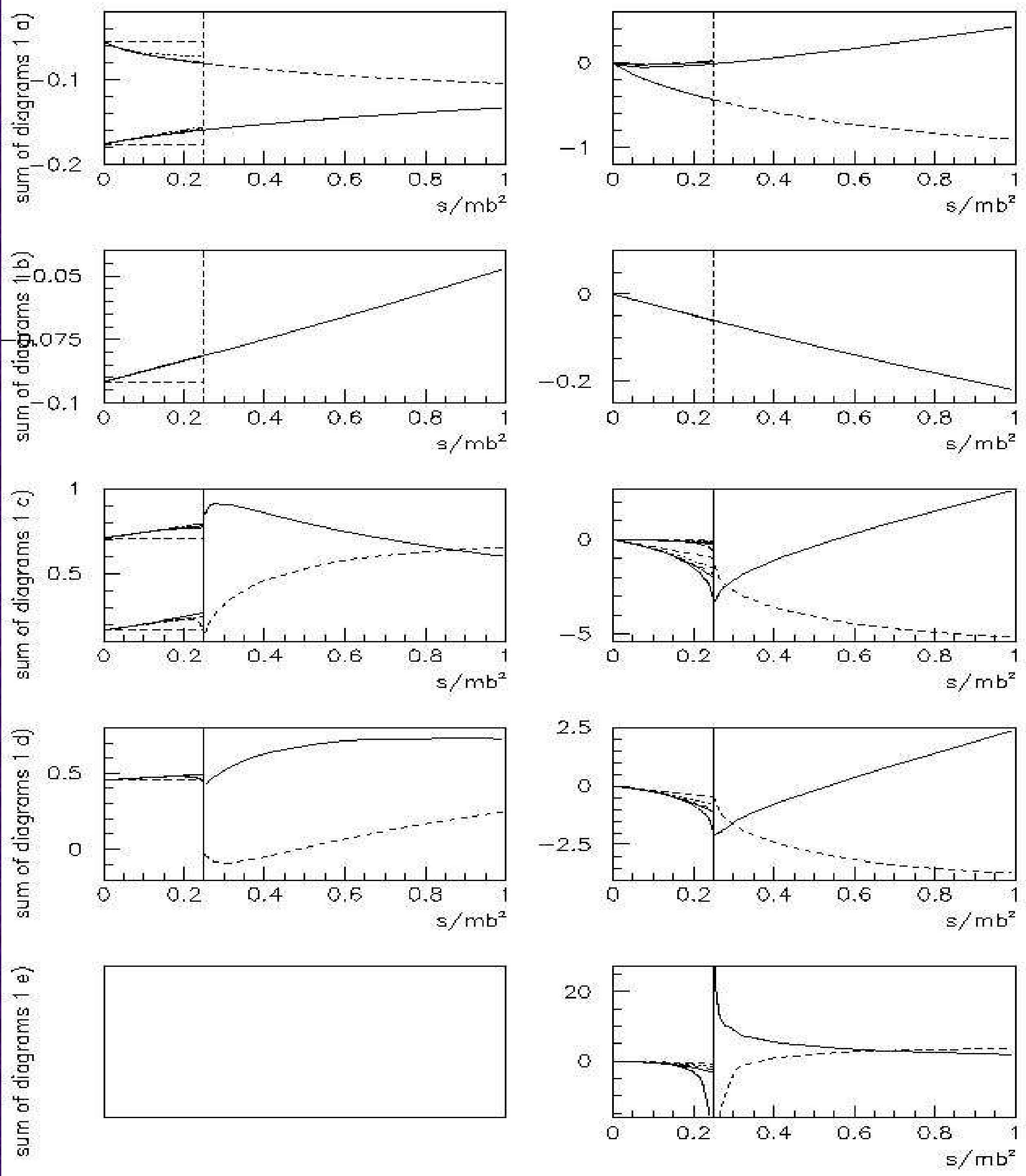

Four form factors: $f^7{}_{1,}$ $f^7{}_{2,}$ $f^9{}_{1,}$ $f^9{}_2$

f72

mc/mb = 0.25
mu = 4.3 GeV

s/mb^2	real	imag	+/- real	+/- imag	Asatryan *et al*.	% difference
0	-4.6091	-0.683291	0.00449565	0.00241093	(4.60379 , 0.68510)	(0.11 , 0.26)
0.025	-4.6494	-0.722156	0.00451309	0.00242645	(4.64343, 0.72521)	(0.13 , 0.42)
0.05	-4.6896	-0.760544	0.00457602	0.00243797	(4.68330 , 0.76313)	(0.13 , 0.34)
0.075	-4.7297	-0.79845	0.00468541	0.00244627	(4.72256 , 0.80146)	(0.15 , 0.37)
0.1	-4.7667	-0.836902	0.0046691	0.00231983	(4.76072 , 0.84073)	(0.12 , 0.46)
0.125	-4.8014	-0.875057	0.00469182	0.00236853	(4.79738 , 0.88118)	(0. , 0.69)
0.15	-4.8313	-0.91161	0.00471217	0.0024479	(4.83214 , 0.92295)	(0. , 1.2)
0.175	-4.8535	-0.943052	0.0047396	0.00249432	(4.86460 , 0.96614)	(0.23 , 2.4)
0.2	-4.8629	-0.961195	0.00479811	0.0025134	(4.89438 , 1.01082)	(0.6 , 4.9)
0.225	-4.8486	-0.940152	0.00473093	0.00251089	(4.92111 , 1.05702)	(1.5 , 11.)
0.25	-4.7695	-0.667815	0.00469771	0.00237495		
0.275	-5.3392	-0.759364	0.00527892	0.00374862		
0.3	-5.4917	-0.965272	0.00541578	0.00363222		
0.325	-5.5802	-1.15024	0.00551671	0.00331638		
0.35	-5.6311	-1.31817	0.00557455	0.00303262		
0.375	-5.6587	-1.47163	0.00559267	0.00303062		
0.4	-5.6711	-1.61315	0.00557072	0.00301081		
0.425	-5.6724	-1.74402	0.00556811	0.00289102		
0.45	-5.666	-1.86573	0.00560685	0.00302966		
0.475	-5.6534	-1.97888	0.00555897	0.00259011		
0.5	-5.6359	-2.08548	0.00553331	0.00257912		
0.525	-5.6153	-2.18598	0.00548811	0.00244327		
0.55	-5.5917	-2.28045	0.00542625	0.00218765		
0.575	-5.5656	-2.36957	0.005463 0	0.00222488		
0.6	-5.5381	-2.45435	0.00546937	0.00221212		
0.625	-5.5086	-2.53439	0.00544076	0.00212212		
0.65	-5.4786	-2.61097	0.00540994	0.00209547		
0.675	-5.4475	-2.68339	0.00536334	0.00218884		
0.7	-5.416	-2.75308	0.00532535	0.00217397		
0.725	-5.384	-2.8198	0.00529206	0.00208739		
0.75	-5.3512	-2.88307	0.00527202	0.00178694		
0.775	-5.3185	-2.94437	0.00523917	0.00170597		
0.8	-5.2856	-3.00323	0.00520191	0.00170467		
0.825	-5.252	-3.05863	0.00513431	0.00195504		
0.85	-5.2189	-3.11299	0.00509801	0.00204826		
0.875	-5.1858	-3.16548	0.00507216	0.0021225		
0.9	-5.1528	-3.21612	0.00505676	0.00217776		
0.925	-5.1198	-3.26489	0.00505183	0.00221404		
0.95	-5.0869	-3.31181	0.00505736	0.00223133		
0.975	-5.054	-3.35686	0.00507335	0.00222964		
1	-5.0212	-3.40005	0.0050998	0.00220897		

f92 mc/mb = 0.25
mu = 4.3 GeV

s/mb^2	real	imag	+/- real	+/- imag	Asatryan *et al*.	% difference
0	0.00415	0.00766951	1.80E-05	-6.92E-06	(0,0)	extrap. remnant
0.025	-0.7526	0.11762	0.000897499	0.000401576	(-0.79209 , 0.11998)	(5.25 , 1.98)
0.05	-1.7256	0.198357	0.00194637	0.00087404	(-1.76441 , 0.196275)	(2.19 , 1.06)
0.075	-2.9144	0.249838	0.00316606	0.00141091	(-2.95112 , 0.24967)	(1.24 , 0.068)
0.1	-4.4214	0.27928	0.00431807	0.00193577	(-4.40730 , 0.28243)	(.03 , 1.12)
0.125	-6.3895	0.281839	0.00667766	0.00251137	(-6.20023 , 0.29380)	(3.05 , 4.07)
0.15	-9.0763	0.24853	0.00919067	0.00314691	(-8.40847 , 0.28156)	(7.94 , 11.7)
0.175	-13.063	0.158923	0.0126042	0.00435561	(-11.1216 , 0.24256)	(17.5 , 34.5)
0.2	-19.886	-0.0351899	0.020051	0.00524091	(-14.4401 , 0.17292)	(37.7 , 79.6)
0.225	-35.945	-0.534399	0.0357038	0.00658227	(-18.4754 , 0.06812)	(94.5 , 684.)
0.25	-259.79	-22.5461	0.0260258	0.0389505		
0.275	24.0428	-36.675	0.048981	0.0355856		
0.3	18.8165	-28.0231	0.0479266	0.0338189		
0.325	15.9367	-22.7579	0.0452504	0.03565		
0.35	14.4611	-20.2111	0.0435452	0.037016		
0.375	13.6467	-18.791	0.042618	0.028065		
0.4	13.2124	-17.9447	0.0419445	0.0280196		
0.425	13.0223	-17.4254	0.0413432	0.026879		
0.45	13.0015	-17.1069	0.0406705	0.0259676		
0.475	13.1027	-16.9188	0.0407548	0.0254777		
0.5	13.3012	-16.8188	0.0404835	0.0229141		
0.525	13.5684	-16.7663	0.0403834	0.0211088		
0.55	13.9027	-16.7592	0.0404542	0.021792		
0.575	14.2833	-16.7773	0.0405738	0.0229638		
0.6	14.6985	-16.8062	0.0404412	0.0246621		
0.625	15.1536	-16.8517	0.0399077	0.0251284		
0.65	15.6305	-16.8951	0.0395879	0.0255323		
0.675	16.1364	-16.9431	0.0392007	0.0256502		
0.7	16.6588	-16.985	0.0392805	0.0255967		
0.725	17.1998	-17.0224	0.0397416	0.0253535		
0.75	17.7654	-17.0583	0.0410058	0.0246642		
0.775	18.3368	-17.0837	0.0417876	0.0243103		
0.8	18.9202	-17.1017	0.0425017	0.0240396		
0.825	19.5226	-17.1159	0.0431141	0.023771		
0.85	20.1271	-17.1173	0.0437058	0.0236974		
0.875	20.7393	-17.1089	0.0442493	0.0237535		
0.9	21.3594	-17.0908	0.0447448	0.0239395		
0.925	21.9872	-17.0629	0.0451922	0.0242552		
0.95	22.6229	-17.0252	0.0455915	0.0247006		
0.975	23.2663	-16.9779	0.0459427	0.0252759		
1	23.9175	-16.9207	0.0462457	0.0259809		

Conclusions

- Massive 2-loop radiative corrections can be performed reliably with our methods, provided enough computing power.
- Caveat: IR singularities need to be treated separately.
- It would be useful to fully integrate Feynman diagram generation programs (Qgraf, Feynarts…) with the numerical 2-loop algorithm.
- A completely automated interface of various components (diagram generation, computer algebra, numerical integration) will boost productivity and reliability.